

Unveiling the molecular environment of the enigmatic PeVatron candidate LHAASO J2108+5157

I. Toledano–Juárez,^{a,*} E. de la Fuente,^b K. Kawata,^c D. Tafoya,^d M. A. Trinidad,^e M. Yamagishi,^f S. Takekawa,^g M. Ohnishi,^c A. Nishimura,^h T. Onishi,ⁱ S. Kato,^b T. Sako,^b M. Takita,^b H. Sano^j and R. K. Yadav^k

^aDoctorado en Ciencias en Física, CUCEI, Universidad de Guadalajara, Jalisco, México

^bDepartamento de Física, CUCEI, Universidad de Guadalajara, Jalisco, México

^cInstitute for Cosmic Ray Research, University of Tokyo, Kashiwa, Japan

^dDepartment of Space, Earth, and Environment, Chalmers University of Technology, Sweden

^eDepartamento de Astronomía, Universidad de Guanajuato, Guanajuato, México

^fInstitute of Astronomy, Graduate School of Science, The University of Tokyo, Mitaka, Tokyo, Japan

^gDepartment of Applied Physics, Faculty of Engineering, Kanagawa University, Kanagawa, Japan

^hNobeyama Radio Observatory, National Astronomical Observatory of Japan, National Institutes of Natural Sciences, Nagano, Japan

ⁱDepartment of Physics, Graduate School of Science, Osaka Metropolitan University, Sakai, Osaka, Japan

^jFaculty of Engineering, Gifu University, Yanagido, Gifu,

^kNational Astronomical Research Institute of Thailand (Public Organization), Chiangmai, Thailand

E-mail: ivan.toledano9284@alumnos.udg.mx

Abstract. We summarize the results of previous works in which we analyzed the molecular environment around the PeVatron candidate LHAASO J2108+5157, using ^{12,13}CO observations. As specific case, we present evidence that the observed sub-PeV emission is produced in two molecular clouds as cosmic-ray targets ([FKT-MC]2022 and [FTK-MC]) with two different LSR velocities but with the same distances. We recalculate the distance of [FKT-MC]2022, obtaining the value of 1.6 kpc. We suggest that both clouds are part of the same structure, where [FTK-MC] is blueshifted with respect to [FKT-MC]2022 favoring gravitational collapse and star formation.

Keywords: PeVatrons—Individual: LHAASO J2108+5157—Molecular lines: CO

38th International Cosmic Ray Conference (ICRC2023)
26 July - 3 August, 2023
Nagoya, Japan



*Speaker.

1. Introduction

PeVatrons are astronomical objects that act as natural particle accelerators capable of accelerating cosmic rays (CRs) up to PeV energies. The accelerated CRs can interact with the surrounding environment by hadronic (e.g. neutral pion decay) or leptonic (e.g. inverse Compton scattering) processes, giving place to gamma-ray emission with energies above 100 TeV. Their detection has been possible thanks to gamma-ray observatories such as LHAASO–KM2A [e.g. 1], HAWC (e.g [2]), and Tibet-AS γ (e.g. [3]). While some PeVatrons have already been associated with an astronomical object counterpart, the recently detected sub-PeV gamma-ray source LHAASO J2108+5157 (J2108 hereafter) [1, 4] stands as an exception in this regard. This enigmatic source is located at R.A. (J2000) = $21^{\text{h}}08^{\text{m}}52.8^{\text{s}}$; DEC (J2000) = $+51^{\circ}57'00''$ ($l = 92.30^{\circ}$, $b = 2.84^{\circ}$), towards the direction of Cygnus OB7 molecular cloud, suggesting that its gamma-ray emission is hadronic in nature, in which the accelerated CRs interact with the molecular material in the environment.

In previous works ([5, 6]; hereafter paper I and paper II respectively), we analyzed $^{12,13}\text{CO}$ molecule line emission data towards the vicinity of J2108. Low resolution ($2.7'$) $^{12,13}\text{CO}$ ($J=2\rightarrow 1$) data was obtained with the 1.8m Osaka Prefecture University (OPU) radio telescope (e.g. [7] and references therein), while higher resolution ($17.0''$) $^{12,13}\text{CO}$ ($J=1\rightarrow 0$) data was taken most recently with the 45m radio telescope of Nobeyama Radio Observatory (hereafter NRO-45m; e.g. [8]). Details of the observations and data reduction process are described in paper I (for low-resolution) and paper II (for high-resolution) respectively. CO emission is used as an indirect tracer for molecular hydrogen H_2 , as the latter is not readily observable because of its higher-energy excitation transitions. Because ^{12}CO emission can become optically thick in molecular clouds, it becomes saturated and it is difficult to infer the whole molecular gas properties accurately. On the other hand, ^{13}CO emission could be optically thin, less susceptible to these opacity effects, making it possible to probe the inner regions of the molecular cloud, allowing us to better estimate the CO column density in order to calculate reliable physical parameters. Using archival atomic hydrogen HI 21cm data from the Dominion Radio Astrophysical Observatory (DRAO¹; [9]), we use CO and HI data to estimate the nucleon column density ($N(\text{H}) = N(\text{HI}) + 2N(\text{H}_2)$) in the vicinity of J2108.

In this work we present a summary of the analysis made in Paper I and II for the molecular environment around LHAASO J2108+5157. In Section 2 we describe the molecular clouds that we proposed to be associated with the sub-PeV gamma-ray emission of LHAASO J2108+5157. The results and discussion are presented in Section 3, and the conclusions are summarized in Section 4.

2. Molecular clouds associated with LHAASO J2108+5157

J2108 was previously associated with the molecular cloud [MML2017]4607 [4] of the catalog of [10], detected by ^{12}CO ($J=1\rightarrow 0$) with a LSR velocity (V_{LSR}) of $\sim -13 \text{ km s}^{-1}$. In paper I we proposed the molecular cloud [FKT-MC]2022 ($V_{\text{LSR}} \sim -3 \text{ km s}^{-1}$) to be another candidate to produce the observed sub-PeV gamma-ray emission of J2108. This proposed molecular cloud was detected using optically thick OPU ^{12}CO ($J=2\rightarrow 1$) emission and its physical parameters were estimated considering optically thin OPU ^{13}CO ($J=2\rightarrow 1$) emission. However, the sensitivity

¹DRAO is part of the Canadian Galactic Plane Survey Project (CGPS). <https://www.cadc-ccda.hia-ihp.nrc-cnrc.gc.ca/en/search/#resultTableTab>

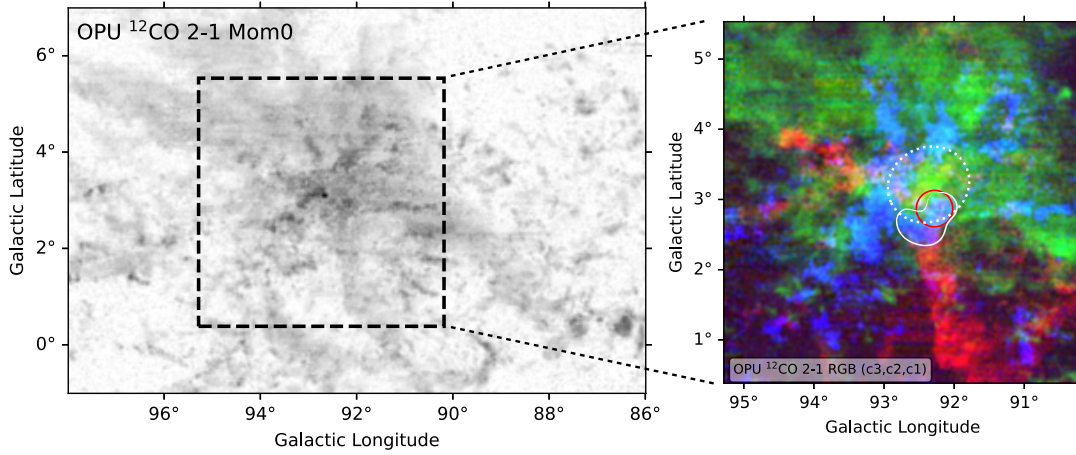


Figure 1: Molecular clouds associated to J2108. **Left:** Moment 0 map of the FOV of OPU ¹²CO (J=2→1) observations towards Cygnus OB7 association [5], integrated between -100 and 80 km s⁻¹. The angular resolution of the map is ~ 3'. **Right:** RGB image as an inset of the left panel, in the vicinity of J2108. Colors show moment 0 maps associated with spectral components (see main text for details) C₃ (red), C₂ (green), and C₁ (blue), respectively. The red circle correspond to the 95% upper limit (radius 0.26 deg) of LHAASO J2108+5157. White dotted and solid lines denote the extension of molecular clouds [FKT-MC]2022 and FTK-MC, respectively.

of the ¹³CO (J=2→1) OPU observations was not enough to study the spectral component at $V_{\text{LSR}} \sim -13 \text{ km s}^{-1}$ in the optically thin regime. In paper II, we used recent NRO-45m data to characterize a molecular cloud, labeled as [FTK-MC] ($V_{\text{LSR}} \sim -13 \text{ km s}^{-1}$) for the first time in the optically thin regime, which showed a remarkable agreement in morphology with *Fermi*-LAT data above 2 GeV associated with J2108 high energy (HE) gamma-ray counterpart 4FGL J2108.0+5155, reported by [11].

3. Results and Discussion for [FKT-MC]2022 and [FTK-MC]

In the left panel of Fig. 1 we present a moment 0 map of the field of view (FOV) of the OPU ¹²CO (J=2→1) emission. In the vicinity of J2108, the molecular line emission presents three main spectral components, that we denote as C₁, C₂, and C₃ (paper II), with LSR velocities of -13, -3 and +9 km s⁻¹, respectively. To analyze each spectral component separately, we computed three moment 0 maps considering the following LSR velocity ranges: -20 to -8 km s⁻¹, -5 to -0 km s⁻¹, and 5 to 12 km s⁻¹, associated with spectral components C₁, C₂, and C₃, respectively. In Fig. 1, we visually present the emission from each spectral component in a RGB image. The 95% upper limit (UL) of J2108 is denoted by a red circle, which intersects with the extension of the molecular clouds [FKT-MC]2022 and [FTK-MC], denoted by white dotted and solid lines, respectively.

Tab. 1 provides the position, V_{LSR} , and size of [FKT-MC]2022, which is associated with spectral component C₂, and is surrounded by molecular gas associated with component C₁. Given the probability that both components correspond to molecular gas located at a similar distance (see Section 3.1), this could be indicating that [FKT-MC] might lie in a cavity within the molecular cloud.

In the top panels of Fig. 2, we present an RGB image obtained from the NRO-45m ^{12}CO ($J=1\rightarrow 0$) and ^{13}CO ($J=1\rightarrow 0$) data, illustrating the same spectral components. The molecular cloud [FTK-MC] is delimited by a white solid line. However, it is important to note that the FOV of the NRO-45m observations does not cover all the extension of [FKT-MC]2022. In the corresponding bottom panels, we display components C_1 and C_2 as contours, in combination with a TS map adapted from Fig. 3 of [11]. The TS map was generated using *Fermi*–LAT data above 2 GeV. The NRO-45m observations, with their higher resolution, reveal that [FTK-MC] has two substructures, namely [FTK-MC]J2108 and [FTK-MC]HS, depicted as dashed and dotted ellipses, respectively. These substructures are named based on their proximity to the positions of J2108 and HS, the latter being a HE gamma-ray source with a hard photon index, not included in the 4FGL catalog, and proposed by [11]. For reference, Tab. 1 provides the positions, V_{LSR} , and sizes of both [FTK-MC]J2108 and [FTK-MC]HS. Considering both substructures, we estimated the overall size of [FTK-MC] to be ~ 0.55 degrees, as detailed in paper II.

As previously mentioned, there is a remarkable correlation between the *Fermi*–LAT data and the distribution of CO emission, particularly in the region of [FTK-MC], which is associated with spectral component C_1 . Notably, the CO emission is the brightest near the peak of the *Fermi*–LAT TS map. Additionally, it appears that the molecular gas linked to [FKT-MC]2022 seems to also trace, albeit in a lesser extent, the upper leftmost part of the extended *Fermi*–LAT data, in particular with the $^{13}\text{CO}(J=1\rightarrow 0)$. This intriguing correlation may indicate the possibility that the gamma-ray emission results from the interaction (hadronic) between accelerated CRs and the molecular material of both clouds.

3.1 Distance, physical parameters, and hadronic modeling

To estimate reliable physical parameters of the molecular cloud associated with J2108, having a good estimate of the distance is essential. In a previous study of [4], J2108 was associated with the molecular cloud [MML2017]4607. The reported distance of 3.28 kpc for this cloud was estimated using the kinematic distance method via the rotation curve model of Brand & Blitz [12].

However, in paper II, we adopted a different approach employing the Bayesian calculator and the algorithms of [13]. This method takes the V_{LSR} and position of a source as inputs, and subsequently determines a distance probability density function. It considers various factors, such as the probable association with nearby sources that have a distance determined through parallax measurements, the spiral arms of the Milky Way, or even the kinematic distance. The inputs and results of these calculations are summarized in Tab. 1.

The results show that it is most likely that the molecular gas associated with component C_1 and C_2 is located at a similar distance of ~ 1.6 kpc, strongly influenced by the accurate measurement of the distance (1.63 kpc) to the nearby source G092.69+3.08 (with coordinates $l=92.671^\circ$, $b=3.071^\circ$, and $V_{\text{LSR}} = -5.0 \text{ km s}^{-1}$). If we remove G092.69+3.08 from the parallax catalog used in the algorithm, the most probable distance of the molecular gas associated with the spectral component C_1 shifts to ~ 2.8 kpc, based on the determination of the kinematic distance for the source. On the other hand, the molecular gas associated with component C_2 is estimated to be at a distance of ~ 1.3 kpc, associated with the Local Arm of the Milky Way. Moreover, in both scenarios, it remains most probable that the molecular gas linked to the spectral component C_3 is associated with the Local Arm, at a distance of ~ 1.2 kpc.

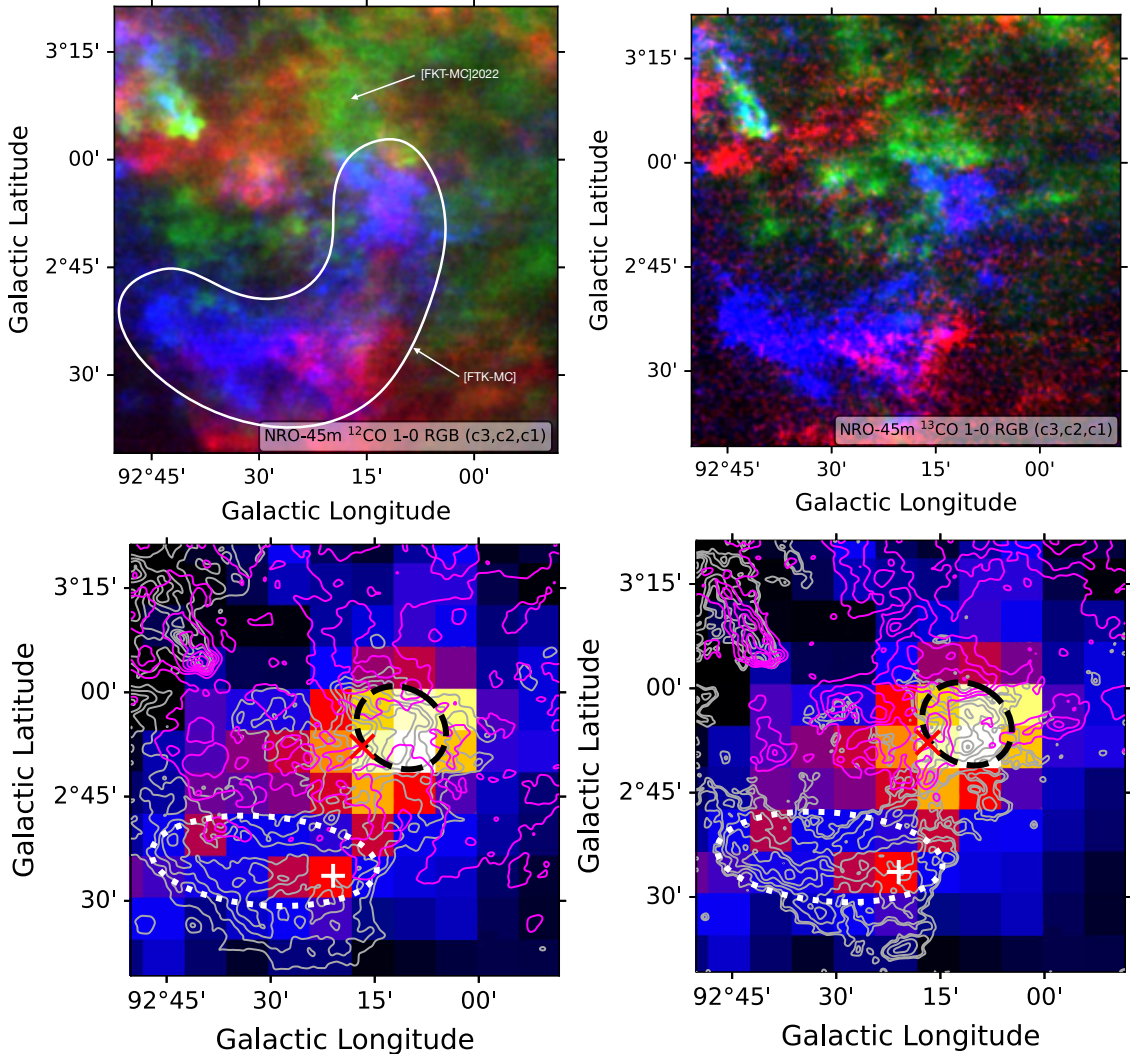


Figure 2: NRO-45m ^{12}CO ($J=1\rightarrow 0$) and ^{13}CO ($J=1\rightarrow 0$) observations. **Top:** RGB image of the spectral components of ^{12}CO (left) and ^{13}CO (right). The colors represent moment 0 maps integrated in the same LSR velocity ranges as right panel of Fig. 1. **Bottom:** *Fermi*-LAT TS map in color scale, adapted from Fig. 3 of [11], with $^{12}\text{CO}(J=1\rightarrow 0)$ (left) and $^{13}\text{CO}^{12}\text{CO}(J=1\rightarrow 0)$ (right) moment 0 maps for spectral component C_1 (grey) and C_2 (magenta) overlaid as contours. The contours are $[-4,4,5,8,12,16,20]$ times the rms value of 0.5 K km s^{-1} and $[-4,4,5,6,7,8]$ times 2.5 K km s^{-1} for the ^{13}CO ($J=1\rightarrow 0$) emission component C_1 and C_2 , respectively. The dashed black ([FKT-MC]2023/J2108) and white dotted ([FKT-MC]2023/HS) ellipses braces the two regions where the physical parameters were determined. The x and the cross indicate the central position of J2108 and HS respectively.

After careful consideration and taking into account the agreement in morphology between the molecular material from both clouds and the *Fermi*-LAT data, the estimated distance of 1.6 kpc is adopted for both [FKT-MC]2022 and [FTK-MC]. This choice is further supported by the fact that this estimated distance lies within the range of celestial features in the Cygnus constellation, from 600 pc (North American and Pelican Nebula) to 1.7 kpc (Cygnus X, [14]). This consideration opens the possibility that [FKT-MC]2022 and [FTK-MC] are part of the same large-scale molecular

Table 1: Estimation of the distance D to the molecular clouds [FKT-MC]2022 and [FTK-MC] using the Bayesian distance calculator of [13]. We present the probability P of association to a parallax measured source, the local galactic arm, or using the kinematic distance method, and their corresponding reference.

Cloud Name	l [deg]	b [deg]	Size [deg]	V_{LSR}^{**} [km s $^{-1}$]	D [kpc]	P	Association	Reference
[FKT – MC]2022	92.40	3.20	1.10±0.20	-2.9±0.1	1.6±0.1	0.59	Parallax	BeSSeL Survey [15]
[FTK – MC]J2108	92.20	2.90	0.34±0.01	-11.6±0.5	1.6±0.1	0.52	Parallax	BeSSeL Survey [15]
[FTK – MC]J2108	92.20	2.90	0.34±0.01	7.2±0.5	1.2±0.3	0.50	Local Arm	BeSSeL Survey [15]
[FTK – MC]J2108*	92.20	2.90	0.34±0.01	-11.6±0.5	2.7±0.7	0.47	Kinematic distance	Rotation curve [16]
[FTK – MC]HS	92.53	2.59	0.21±0.01	-13.2±0.5	1.6±0.1	0.43	Parallax	BeSSeL Survey [15]
[FTK – MC]HS	92.53	2.59	0.21±0.01	8.8±0.5	1.2±0.3	0.46	Local Arm	BeSSeL Survey [15]
[FTK – MC]HS*	92.53	2.59	0.21±0.01	-13.2±0.5	2.9±0.7	0.58	Kinematic distance	Rotation curve [16]

* Without considering G092.69+3.08 in the parallax sources catalog.

** The V_{LSR} of the sources were obtained using the corresponding ^{13}CO emission (Paper I and II).

Table 2: Physical parameters for the molecular clouds [FKT-MC]2022 and [FTK-MC], estimated using optical thin ^{13}CO emission.

Cloud Name	Distance [kpc]	$N(\text{H})^a$ [10^{21} cm^{-2}]	$n(\text{H})^{a,b}$ [cm^{-3}]	Size [deg]	$M(\text{HI} + \text{H}_2)$ [$10^3 M_{\odot}$]	T_{exc} [K]	W_p [10^{47} erg]	Cutoff [TeV]
[FKT-MC]2022	1.6±0.1	3.7±0.7	78±15	1.1±0.1	4.3±1.6	7.2±0.1	1.8 ± 0.6	600 $^{+400}_{-200}$
[FTK – MC]	1.6±0.1	6.2±2.1	133±45	0.55±0.02	7.5±2.9	8.4±0.6	1.1 $^{+0.5}_{-0.3}$	600 $^{+300}_{-300}$

^a The column and number density of nucleons is calculated as $N(\text{H}) = 2N(\text{H}_2) + N(\text{HI})$ and $n(\text{H}) = 2n(\text{H}_2) + n(\text{HI})$, respectively.

^b The angular depth of [FTK-MC] of 0.55 deg was used for the estimation of the nucleon number density $n(\text{H})$ of [FKT-MC]2022.

structure, where the gamma-ray emission originates particularly in the region of these molecular clouds. A possible scenario could be that global gravitational collapse is occurring in the molecular complex [17], and the gas associated with the spectral component C_1 is tracing blueshifted molecular material (see Fig. 1) around the systemic velocity of $\sim -4 \text{ km s}^{-1}$ for Cygnus OB7 [18], but a more detailed kinematic study is necessary to better constrain the 3d morphology of the region.

Extracting the corresponding $^{12,13}\text{CO} (J=2 \rightarrow 1)$ and $^{12,13}\text{CO} (J=1 \rightarrow 0)$ spectra from the regions of [FKT-MC]2022 and [FTK-MC], respectively, in addition to the DRAO HI 21 cm data, we estimate the physical parameters of the molecular clouds using the methods and considerations presented in Paper I and II. Assuming spherical symmetry, we consider a depth of 0.55 deg for [FTK-MC] (paper II). Given that the size of [FTK-MC] was computed using better constrained optically thin $^{13}\text{CO}(J=1 \rightarrow 0)$ emission, we decide to use the same value for the depth of [FKT-MC]2022, for consistency. The nucleon number density $n(\text{H})$ was computed using the estimated distance of $\sim 1.6 \text{ kpc}$ to both sources. These consideration were not taken for [FKT-MC]2022 in Paper I. The derived physical parameters are listed in Tab. 2.

The Naima² [19] package (version 0.10.0) in Python was employed to fit the spectra energy distribution (SED) of J2108 [4] at sub-PeV energies (see Fig. 3), considering the neutral pion decay hadronic process and using the obtained distance and nucleon number densities for both [FKT-MC]2022 and [FTK-MC] as input parameters. The hadronic modeling considers an exponential

²<https://naima.readthedocs.io/en/latest/index.html>

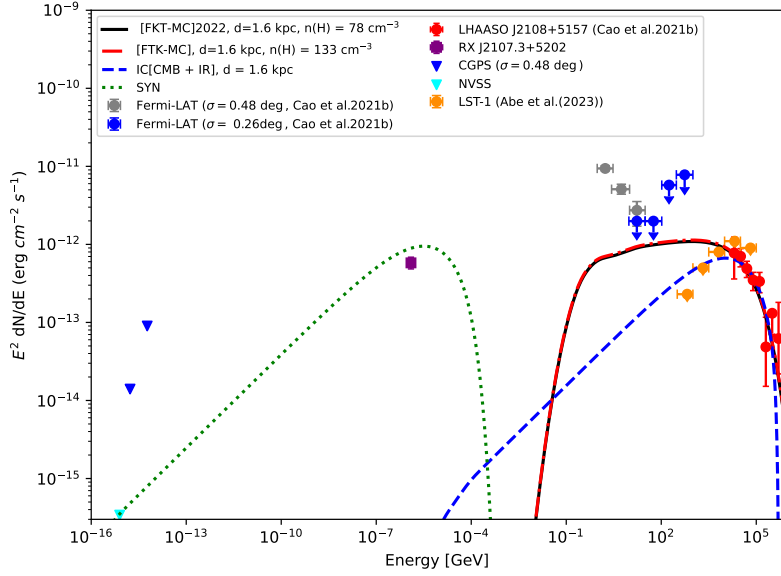


Figure 3: Spectral energy distribution of the LHAASO J2108+5157. The solid black and dashdotted red curves correspond to the hadronic modeling using the physical parameters of [FKT-MC]2022 and [FTK-MC], respectively. The green dotted curve is the spectral energy distribution expected from synchrotron radiation. The blue dashed curve represents the expected spectral energy from the inverse Compton effect, considering a CMB and IR seed photon field. We add the flux points of LST-1 reported by [11], shown as orange circles. For more details see Fig. 8 of Paper I.

cutoff power law spectrum with a fixed spectral index of 2.0 [4]. The total required energy W_p and the energy cutoff of the cosmic ray proton population to reproduce the observed SED of J2108 are shown in Tab. 2 for each molecular cloud. A similar $W_p \sim 1.5 \times 10^{47}$ ergs is obtained for [FKT-MC]2022 and [FTK-MC], in agreement with what was reported in Paper II, and an order of magnitude lower than the value of 2×10^{48} ergs obtained by [4]. A similar value of W_p could suggest that the molecular environments of both molecular clouds could contribute in a similar way to the observed sub-PeV gamma-ray emission, favouring the argument that both clouds are located at a similar distance and are part of a same molecular structure.

We present the fitted SED of J2108 in Fig. 3, considering both hadronic (neutral pion decay) and leptonic (inverse Compton scattering) processes in the modelling. The leptonic modelling uses the same considerations of [4]. A total required energy of $W_e \sim 8.5 \times 10^{46}$ ergs for the electron population to reproduce the observed SED of J2108. The single-component hadronic model does not fully explain the observed SED presented in Fig. 3, so a leptonic contribution to the emission is not excluded.

4. Conclusions

In the following, we summarize the conclusions that we obtain from the OPU and NRO-45m $^{12,13}\text{CO}$ observations towards the vicinity of the PeVatron candidate LHAASO J2108+5157:

- We propose two molecular clouds, [FKT-MC]2022 and [FTK-MC] to produce the observed

sub-PeV gamma-ray emission for LHAASO J2108+5157, favouring a hadronic origin of the emission.

- [FKT–MC]2022 and [FTK–MC] are part of a same molecular structure located at a distance of ~ 1.6 kpc. An average nucleon number density $n(\text{H}) = 2n(\text{H}_2) + n(\text{HI})$ of $\sim 105 \text{ cm}^3$ is estimated between both clouds, considering optically thin ^{13}CO emission. An average required energy of the CR proton population of $W_p \sim 1.5 \times 10^{47}$ ergs is obtained to reproduce the observed SED of LHAASO J2108+5158 at sub-PeV energies, considering a hadronic scenario.

Acknowledgments

The research summarized in this article was supported by the Inter-University Research Programme of the Institute for Cosmic Ray Research (ICRR), University of Tokyo (UTokyo), grant 2023i–F–005. EdelaF thanks the ICRR-UTokyo staff for several support during Sabbatical stay in 2021, and several academic stays between 2022 and 2023. IT–J gratefully acknowledges support from the Consejo Nacional de Ciencias y Tecnología, México grant 754851, and the Onsala Space Observatory during an academic visit in 2023. The authors are grateful for computational resources and technical support from the Centro de Análisis de Datos y Supercómputo of the Universidad de Guadalajara through the Leo-Atrox supercomputer.

References

- [1] Cao, Z., et al. 2021a, *Nature*, 594, 33
- [2] Abeysekara, A.U, et al. 2023, *Nucl. Instrum. Methods Phys. Res. A.*, 1052, 168253
- [3] Amenomori, M., et al., 2021c, *PRL*, 127, 031102
- [4] Cao, Z., et al. 2021b, *ApJL*, 919, L22
- [5] de la Fuente, E, Toledano–Juárez, I., Kawata, K., et al. 2023a, *PASJ*, 75, 546 (paper I)
- [6] de la Fuente, E, Toledano–Juárez, I., Kawata, K., et al. 2023b, *A&A*, 275, L5 (paper II)
- [7] Nishimura, A., Tokuda, K., Kimura, K., et al. 2020, *Proc. SPIE*, 11445, 114457F1-114457F13
- [8] Minamidani, T., Nishimura, A., Miyamoto, Y., et al. 2016, *Proc. SPIE*, 9914, 99141Z
- [9] Taylor, A. R., Gibson, S. J., Peracaula, M., et al. 2003, *AJ*, 125, 3145
- [10] Miville-Deschenes, M.-A., Murray, N., & Lee, E. J. 2017, *ApJ*, 834, 57
- [11] Abe, S., Aguasca-Cabot, A., Agudo, I., et al., 2023, *A&A*, 673, A75.
- [12] Brand J., Blitz L., 1993, *A&A*, 275, 67
- [13] Reid, M. J., Menten, K. M., Brunthaler, A. et al. 2019, *ApJ*, 885, 131
- [14] Schneider N., et al., 2006, *Astron. Astrophys.*, 458, 855
- [15] Xu, Y., Li, J. J., Reid, M. J., et al. 2013, *ApJ*, 769,15
- [16] Reid M. J., et al., 2014, *ApJ*, 783, 130
- [17] Snell R. L., Loren R. B., 1977, *ApJ*, 211, 122.
- [18] Dobashi K., Shimoikura T., Endo N., et al., 2019, *PASJ*, 71, S11.
- [19] Zabalza V., 2015, *ICRC*, 34, 922